Atmos. Chem. Phys. Discuss., 8, 12053–12079, 2008
www.atmos-chem-phys-discuss.net/8/12053/2008/

Atmospheric Chemistry and Physics Discussions

Characterizing ozone production and response under different meteorological conditions in Mexico City

W. Lei[1,2], M. Zavala[1,2], B. de Foy[1,3], R. Volkamer[2,4], and L. T. Molina[1,2]

[1]Molina Center for Energy and the Environment, CA, USA
[2]Department of Earth, Atmospheric and Planetary Sciences, Massachusetts Institute of Technology, MA, USA
[3]Department of Earth and Atmospheric Sciences, Saint Louis University, MO, USA
[4]Department of Chemistry and Biochemistry, University of Colorado at Boulder, CO, USA

Received: 9 May 2008 – Accepted: 20 May 2008 – Published: 18 June 2008

Correspondence to: L. T. Molina (ltmolina@mit.edu)

Published by Copernicus Publications on behalf of the European Geosciences Union.

Abstract

Tropospheric photochemistry, particularly the formation of ozone (O_3), depends not only on pollutant emissions, but also on meteorological conditions. In this study a 3-D chemical transport model CAMx was employed to investigate the O_3 formation and its response to emission reductions under three distinctively different meteorological conditions ("Cold Surge", "O_3-North" and "O_3-South") in the Mexico City Metropolitan Area during the MCMA-2003 field measurement campaign. The O_3 formation characteristics and sensitivity to emissions changes were found to be weakly dependent on the meteorological conditions. The evolution of O_3 formation and sensitivity were also examined along the photochemical plume transport pathway. The midday O_3 production was found to undergo a rapid increase in a narrow range of chemical aging, while plumes in the downwind were characterized with low and constant O_3 production, and plumes along their transport pathway were featured by a combination of the two. The O_3 formation was more VOC sensitive near the source area, but as the plume became chemically aged, O_3 formation became progressively VOC insensitive and more NO_x sensitive.

1 Introduction

The photochemistry in the troposphere, particularly the formation of ozone (O_3), is affected not only by the pollutant precursors and their chemical aging (Liu et al., 1987; Sillman, 1999), but also by meteorology (Solomon et al., 2000; Seaman 2000). For example, elevated O_3 episodes are often associated with warm and stagnant meteorological conditions (NRC, 1991). Recently, Baertsch-Ritter et al. (2004) and Dawson et al. (2007) investigated the effects of various meteorological parameters on the O_3 concentrations in the eastern US and Europe using chemical transport models; they found that there were important links between changes in meteorology and O_3 concentrations, such as air temperature having the largest positive effects on O_3 concentration,

and increased wind speeds and mixing height leading to the decrease in O_3. In addition, Dawson et al. (2007) found the nonlinear effects of meteorological parameters on O_3, while Baertsch-Ritter et al. (2004) found that meteorological parameters affect the sensitivity of O_3 formation to nitrogen oxides (NO_x) and volatile organic compounds (VOCs).

As the most populous city in North America, the Mexico City Metropolitan Area (MCMA) exhibits degradation of air quality experienced by many megacities around the world (Molina and Molina, 2002; Molina and Molina, 2004). The extensive MCMA-2003 field campaign was conducted in April 2003 in the MCMA to improve our understanding of air pollution in megacities (Molina et al., 2007). The meteorological conditions during the campaign were identified and classified into three categories: "O_3-South", "O_3-North" and "Cold Surge" by de Foy et al. (2005). These circulation patterns, shown in Fig. 1, were the results of the interactions of synoptic and local circulations. The "O_3-South" episode features a weak synoptic forcing associated with an anticyclone, and thermally driven circulations leads to high O_3 in the south of the city; the "O_3-North" episode features westerlies associated with weak anticyclone conditions to the south and a strong sub-tropical jet to the north of the MCMA, resulting in high O_3 in the north of the city; the "Cold Surge" episode characterizes cold northerlies from the Gulf that brings cold humid air to the Mexico plateau, leading to afternoon convection and rainfalls in the MCMA and high O_3 in the city center due to stable conditions. These meteorological conditions are also frequent in the MCMA in other years (de Foy et al., 2007).

Using a 3-D chemical transport model, CAMx 4.03 (Environ, 2003), we have previously examined the characteristics of photochemical O_3 formation and its response to precursors in the MCMA under the "O_3-South" episode (Lei et al., 2007). In this study, we extend the examinations to the other two meteorological events, "O_3-North" and "Cold Surge", and compare with those obtained under the "O_3-South" episode. In addition, we have investigated the evolutions of O_3 formation and response of the urban plume. One of our goals is to investigate whether and how these characteris-

tics (such as the O_3 formation–precursor–radical relationship and the response of O_3 formation to changes in emissions) change under different meteorological conditions. If the NO_x/VOC chemistry of O_3 formation behaves consistently under different meteorological conditions, the formulation of emissions control strategies would be greatly facilitated. Another goal is to explore how the characteristics of O_3 formation and its sensitivity evolve as the urban plume transports outside of the city, which has important implications for the regional air quality impacts of the urban plumes. Section 2 gives a brief description of the method. Section 3 presents the evaluation of emission uncertainty, model performance, characteristics of O_3 formation and its response to precursors, the chemical evolution of O_3 formation and its sensitivity. A summary of conclusions is provided in Sect. 4.

2 Methodology

The 3-D chemical transport model CAMx 4.03 (Environ, 2003) was again employed in this study. The configurations of model and modeling domain were the same as described in Lei et al. (2007). The meteorological input for the model was generated by MM5 (de Foy et al., 2006). The vertical diffusivity fields (k_v) were reconstructed from the state variables of the MM5 output using the CMAQ algorithm (Byun, 1999). de Foy et al. (2007) found that the CMAQ scheme excessively estimates k_v values. Accordingly we downscaled k_v to 20–30% based on comparison of modeled CO, NO_y and their ratios with observations.

The emission input fields were constructed based on the official emissions inventories (EI) for the years 2002 and 2004 for the MCMA (CAM, 2004, 2006), and were adjusted based on measurements of CO, NO_y and speciated VOCs (see Sect. 3.1).

In addition to the continuous measurements of a few critical pollutants by the monitoring stations of the Ambient Air Monitoring Network of Mexico City (RAMA) (SIMAT, 2003), an extensive array of ground measurements for VOCs were made during the MCMA-2003 campaign, which included speciated VOC measurements from canister

sampling analyzed by Gas Chromatography/Flame Ionization Detection (GC/FID) at various sites (Velasco et al., 2007) and long-path Differential Optical Absorption Spectroscopy (DOAS) measurements of aromatics and formaldehyde at the campaign supersite CENICA (Volkamer et al., 2005). The model performance and the evaluation of the emission uncertainty were evaluated against these ground measurements,i.e., CO, NO_y and O_3 were compared with the RAMA data, VOCs were compared with the GC-FID and DOAS datasets; furthermore the estimates of HCHO emissions were examined against measured emissions from vehicle fleets (Zavala et al., 2006). The performance and emission evaluation will be presented in the next section.

The simulation periods selected were 8–11 April 2003, which was characterized as a "Cold Surge" episode, and 25–30 April 2003, which was an "O_3-North" episode (de Foy et al., 2005). Simulations started one day earlier for each period allowing 24 h for spin-up.

3 Results and discussions

3.1 Evaluation of emission inventory

Lei et al. (2007) evaluated the uncertainties in the official EI using the RAMA data, VOC dataset from the canister sampling coupled with the GC/FID analysis, and the DOAS measurements at CENICA during 13–15 April 2003. In this work, we extended the evaluation using a VOC dataset with a broader spatial and temporal coverage. The GC/FID measurements used in this study included data obtained at CENICA, Pedregal and La Merced during the MCMA-2003 by research groups from Washington State University (WSU) and the Mexican Petroleum Institute (IMP) (Velasco et al., 2007); the aromatics and HCHO concentrations measured with DOAS covered the selected simulation periods at CENICA. Following the evaluation procedure of Lei et al. (2007), a series of simulations with adjusted emissions were conducted, and simulated concentrations were compared with measurements until a satisfactory agreement was reached for CO,

NO_y and speciated VOC concentrations. Figure 2 gives an example of the VOC comparisons after the emissions were adjusted, which shows a good agreement between simulated and measured speciated VOCs. Table 1 summarizes the emission adjustment factors, which shows that the emission estimates for CO and NO_x in the official EIs are accurate (within 10%); the emissions of most alkanes are underestimated by about a factor of 2–4 while the most active alkanes (C7 or above, denoted as ALK5 in Table 1) are overestimated by about a factor of 2; emissions of alkenes are generally accurate, and the emissions of aromatics are probably slightly underestimated by 10–30%. The overestimate of alkanes of C7 or above is probably an artifact due to their low concentrations, which may impose a larger uncertainty in the measurement, and due to the fact that some significant species may not be detected in the measurements. The adjustment range in the table reflects the emission variations in different EI base years and locations. The adjustment factors obtained in this study are consistent with those in Lei et al. (2007), given the variability in different EI years and locations where comparisons were made. The adjusted emissions were then used for the base case run.

It should be noted that even though we have broadened the dataset for the EI evaluations, the VOC comparisons were still made over limited number of sites (CENICA, Pedregal and La Merced) and over a relatively short time period (a few weeks). A more complete identification of the EI uncertainties using this approach requires more measurements with broader spatial and temporal coverage. In addition, direct evaluation of emissions using other measurement techniques (e.g. Kolb et al., 2004; Zavala et al., 2006, Velasco et al., 2007) is needed.

3.2 Performance of O_3 simulation

Figure 3 shows the comparison of measured and simulated near-surface O_3 concentrations in the MCMA urban region during 8–11 ("Cold Surge") and 25–30 ("O_3-North") April 2003. Overall the model reproduced the observations quite well except on some days, such as on 10 and 26 April. Figure 4 shows that on 10 April the simulated O_3

was too high because the simulated northerly component (gap flow) was too weak, leading to the over accumulation of air pollutant plume inside the basin. On 26 April, the photochemical plume in the basin was shifted to the north due to overestimated SW flow (slope flow) in the morning hours, deviating the plume far from the plume's average transport path of this episode. A sensitivity test with an uniform increase of the gap flow by 0.5 m/s (both the northerly and westerly components) between 10:00–17:00 CDT on 10 April dramatically improved the O_3 agreement (Fig. 3); a test with a weakening of the SW slope flow on 26 April (not shown) also significantly improved the O_3 agreement. These results indicate that O_3 concentration on the urban scale is very sensitive to the wind field, and it is essential that the chemical transport model be driven by an accurate meteorological input in the urban scale photochemical modeling. Due to the meteorological and chemical discrepancies, simulated data for 10 and 26 April will not be included for further discussion. Table 2 summarizes the statistical performance for major gaseous pollutants in the MCMA (over 21 RAMA monitoring stations in the urban setting) during each episode (with the exclusion of 10 and 26 April). The various statistical analysis indicate that O_3, CO and NO_y were reasonably well simulated, particularly O_3. It should be noted that during the "Cold Surge" episode the surface O_3 concentration was lower compared to other meteorological conditions. This is because there was a stronger daytime horizontal convection on the "Cold Surge" days. In contrast, CO and NO_y concentrations during the Cold Surge episode were similar to those during the "O_3-North" episode because the mean values of CO and NO_y were weighted more by the concentrations at morning hours and night time when the surface wind was generally calm for all episodes. During the "O_3-South" episode, the O_3 concentration was similar to that of the "O_3-North" episode, but the primary pollutant (CO and NO_y) concentrations were lower than those during other meteorological conditions, which is probably due to reduced emission activities of this episode. The episode of 13–15 April 2003 started on Sunday followed by the Easter Week; anthropogenic emissions were reduced by 10–20% during this episode (Lei et al., 2007) when the residents left the city for holidays.

3.3 Characteristics of O_3 production rate

We examined the net photochemical formation rates of O_x (O_x=O_3+NO_2), $P(O_x)$, and ozone production efficiency (OPE), as a function of NO_x during 8–11, 13–15, and 25–30 April; the results are presented in Fig. 5. For all three meteorological categories, generally $P(O_x)$ increases with increasing NO_x despite various degree of scatter. $P(O_x)$ values are higher during the "O_3-North" and "Cold Surge" episodes than those during the "O_3-South" episode. The lower $P(O_x)$ values in the "O_3-South" episode is due to the reduced emissions as mentioned above, which leads to decreased VOC reactivity and radical production that will be illustrated later. The relatively high values of $P(O_x)$ during the "Cold Surge" episode is probably in part due to the fact that MM5 may not well capture the cloud effects that occurred frequently under this type of meteorological condition, which affect the air mixing (de Foy et al., 2007), and photochemical activities. Despite the high $P(O_x)$ values, the O_3 concentrations during the "Cold Surge" episode are lower than other meteorological conditions (see Table 2, Figs. 3 and 7) due to the stronger advection during this event. During the "Cold Surge" event, there are many data points with high NO_x but low $P(O_x)$, which may be due to the imminent impacts of emissions at some locations (see Fig. 6b below). The values of OPE (concentrating at 5–10 molecules of O_3 per NO_x oxidized) and its dependence on NO_x are similar and consistent under "O_3-South", "O_3-North" and "Cold Surge" conditions, although under the "Cold Surge" condition OPE values appear to be less NO_x-dependent. In summary, the characteristics of $P(O_x)$ and OPE are consistent under all meteorological conditions.

We have analyzed the relationship among $P(O_x)$, VOC reactivity (K_{VOC}), chemical aging (NO_z/NO_y), and primary radical production rate (Q) in the urban area under different meteorological conditions; the results are shown in Fig. 6. The relationship between $P(O_x)$ and K_{VOC} (Fig. 6a) is similar to that of $P(O_x)$-NO_x, indicating the co-emissions of NO_x and VOCs. Figure 6b indicates that in the "Cold Surge" event, the urban plume is more fresh with less chemical processing, which causes the situations

ACPD
8, 12053–12079, 2008

of high NO_x and VOCs but low $P(O_x)$ to occur. The urban air mass is most chemically aged during the "O_3-South" episode with respect to other meteorological conditions, which is understandable considering the dominant flow patterns and terrain setting. As we will see later, chemical aging has significant influences on the NO_x-VOC sensitivity of O_3 formation. $P(O_x)$ is strongly dependent upon the Q term (Fig. 6c), and over 90% of the radicals are removed through the radical-NO_x reactions (Fig. 6d) while less than 10% via the radical-radical reactions, implying that the midday O_3 formation is VOC-limited in the urban area (Sillman, 1995; Kleinman et al., 1997; Daum et al., 2000). Q and K_{VOC} values (which are closely related to each other) are higher during the "Cold Surge" and "O_3-North" episodes than during the "O_3-South" episode, leading to higher $P(O_x)$ values in the former. The lower Q and K_{VOC} values during the "O_3-South" episode are probably due to reduced emissions.

3.4 Response of O_3 production to precursors

We have evaluated the response of O_3 formation to the O_3 precursors by perturbing the emissions and examining the resulting changes in O_3 concentrations and O_3 production rates. The perturbations of emissions include a 50% reduction in NO_x emissions only, a 50 reduction in VOC emissions only, and a 50% reduction in both NO_x and VOC emissions.

Figure 7 illustrates the effects of emissions reductions on surface O_3 in the urban region. It shows that a 50% reduction in NO_x emissions leads to an increase in O_3, while a 50% reduction in VOC emissions leads to a decrease in O_3 by about a factor of 2. In the NO_x 50% reduction scenario, O_3 increases marginally during the "O_3-South" episode, but clearly increases during the other two episodes, most notably during the "Cold Surge" episode. This response behavior is consistent with the chemical aging of the air mass: least aged during the "Cold Surge" days, most aged during the "O_3-South" days, and the "O_3-North" days in between. Another interesting phenomenon occurs in the scenario of the 50% reduction in both NO_x and VOC emissions. During the "O_3-North" episode, the surface O_3 concentrations decreases as in the "O_3-South" case;

however, during the "Cold Surge" episode, the midday O_3 does not change noticeably. This does not mean that O_3 sensitivity chemistry changes during the "Cold Surge" condition against other meteorological conditions, as we will find below.

Figure 8 shows the percentage change of $P(O_x)$ as a function of NO_x from 12:00–17:00 LT during the "Cold Surge" and "North-north" episodes. As in the "O_3-South" case, a 50% reduction in VOCs leads to a significant decrease in $P(O_x)$; a 50% reduction in NO_x leads to a decrease in $P(O_x)$ at low NO_x conditions but an increase in $P(O_x)$ at high NO_x; the 50% reduction in both NO_x and VOC also leads to a decrease in $P(O_x)$ but less than that of the VOC-only reduction case. This is different from the phenomenon for the O_3 concentration showed in Fig. 7. It is because $P(O_x)$ is more relevant to chemistry while O_3 concentration is more dependent on both chemistry and meteorology. The inconsistency in the behaviors of O_3 concentration and $P(O_x)$ suggests that although meteorology may affect the O_3 concentrations significantly, it may not affect O_3 photochemistry as much as the concentration itself. The response of $P(O_x)$ to emission reductions indicates that midday O_3 formation is VOC limited in the urban region, independent of meteorological conditions.

3.5 Evolution of photochemical plume

In order to explore the evolution of a pollution plume as it transports outside of the city and its impact on the regional pollutant levels, we examined the evolution of $P(O_x)$ in a pollutant plume following its pathway during the "O_3-North" event. The "O_3-North" event was chosen because during this event the MCMA urban plume travels a larger space, exerting most environmental impacts at regional scales. Figure 9 shows the evolution of $P(O_x)$ in a plume with three different origins: source area, downwind area, and along the transport pathway. The transport path was approximated by tracking the location of relatively high surface CO concentrations in the plume. We observe that there are distinct relationships of $P(O_x)$-chemical aging (using NO_z/NO_y as the indicator for the photochemical aging) for plumes in the urban center and in the downwind areas. Plumes in the source area are much fresher (indicated by low NO_z/NO_y values), and

as the plumes undergo chemical processing, $P(O_x)$ increases rapidly and reaches very high values within a narrow range of the chemical age. On the other hand, plumes in the downwind area, about 60 km of the source area, are mostly chemically aged, and $P(O_x)$ values are low and nearly constant. Plumes along the transport pathway are featured by the combination of the signatures of fresh plumes (near source) and aged plumes (downwind), this is because as a plume transports, it becomes progressively chemically aged, and meanwhile continuous emissions along the pathway are filled into the plume.

We also investigate the evolution of O_3 formation sensitivity along the plume's transport pathway. Figure 10 shows the percentage of $P(O_x)$ as a function of chemical aging when emissions are reduced (50% in NO_x only, 50% in VOCs only, and 50% both) during 12:00–17:00 LT, 25–30 April, 2003. It can be seen that the O_3 sensitivity changes as the plume evolves. When the plume is fresh, O_3 formation is more VOC sensitive (NO_x depressed); as the plume becomes chemically aged, O_3 formation becomes progressively VOC insensitive and more NO_x sensitive.

4 Conclusions

We have extended the characterization of O_3 formation and its response to emissions changes under "O_3-South" (13–15 April 2003) meteorological condition to two more distinct episodes (8–11 April "Cold Surge" and 25–30 April "O_3-North") using the CAMx model with an improved emissions inventory with greater spatial and temporal coverage. Further, we have examined the evolution of O_3 formation and response using the "O_3-North" episode as a case scenario.

The uncertainty of the MCMA EI was re-evaluated using observed dataset (particularly VOCs) with greater spatial and temporal coverage. The results show that the estimates of CO and NO_x emissions in the MCMA EI are accurate, while VOCs are in general underestimated by a factor of 2–3 (1.6 overall), consistent with the study of Lei et al. (2007). However, even though a larger dataset was used for the EI evalua-

tions, the VOC comparisons were still made over limited locations (CENICA, Pedregal and La Merced) and over a relatively short time period (a few weeks). A thorough identification of the EI uncertainty requires more measurements with a broader spatial and temporal coverage, and measurements from other techniques such as the fleet chasing technique.

By analyzing the relationship among O_x production rate, O_3 precursors and radical source, we found that the characteristics of O_3 formation and its response to emission changes are weakly dependent on meteorological conditions. Under all three meteorological categories, in general midday $P(O_x)$ increases with NO_x with no obvious turnaround behavior, and both midday $P(O_x)$ and OPE values are high at high NO_x conditions compared to those in other urban cities; midday O_3 formation is VOC limited in the MCMA urban region as revealed by both the dependence behavior of $P(O_x)$ on NO_x, VOCs and radical source and the response of $P(O_x)$ to precursor emission reductions.

We have also examined the evolutions of O_3 production and its response to emission reductions during the "O_3-North" event. The plumes in the source region were found to be less chemically aged, and the O_3 production increased rapidly and reached very high values within a short chemical age, while plumes in the downwind area were chemically aged and characterized by low O_3 production; plumes in between were featured by the combination of fresh and aged plumes. In the fresh plume O_3 formation is more VOC sensitive. As the plume becomes chemically aged, O_3 formation becomes progressively VOC insensitive and more NO_x sensitive.

It should be pointed out that in this study, we have covered less-than-a-week simulations for each of the three meteorological episodes. More studies are needed in order to comprehensively characterize the O_3 formation and its response to precursors under various meteorological conditions. We plan to further our modeling studies using the much larger and comprehensive datasets from the 2006 MILAGRO (Megacity Initiative: Local and Global Research Observations) Campaign, in which the meteorology was divided into 6 episode types representing different wind transport (de Foy et al.,

ACPD
8, 12053–12079, 2008

2008), in contrast to the three episode types for MCMA-2003.

Acknowledgements. The authors gratefully acknowledge financial support from the US National Science Foundation (ATM-0528227), Department of Energy (DE-FG02-05ER63980), and the Mexican Metropolitan Environmental Commission (CAM). CAMx is made publicly available by ENVIRON.

References

Baertsch-Ritter, N., Keller, J., Dommen, J., and Prevot, A. S.: Effects of various meteorological conditions and spatial emission reductions on the ozone concentration and ROG/NO_x limitation in the Milan area (I), Atmos. Chem. Phys., 4, 423–438, 2004, http://www.atmos-chem-phys.net/4/423/2004/.

Byun, D. W.: Dynamically consistent formulations in meteorological and air quality models for multiscale atmospheric studies. Part I: Governing equations in a generalized coordinate system, J. Atmos. Sci., 56, 3789–3807, 1999.

CAM (Comisión Ambiental Metropolitana): Inventario de Emisiones 2002 de la Zona Metropolitana del Valle de México, Mexico, 2004.

CAM (Comisión Ambiental Metropolitana): Inventario de Emisiones 2004 de la Zona Metropolitana del Valle de Mexico, Mexico, 2006.

Daum, P. H., Kleinman, L. I., Imre, D. G., Nunnermacker, L. J., Lee, Y.-N., Springston, S. R., Newman, L., and Weinstein-Lloyd, J.: Analysis of the processing of Nashville urban emissions on July 3 and July 18, 1995, J. Geophys. Res., 105, 9155–9164, 2000.

Dawson, J. P., Adam, P. J., and Pandis, S. N.: Sensitivity of ozone to summertime climate in the eastern USA: A modeling case study, Atmos. Environ., 41, 1494–1511, 2007.

de Foy, B., Caetano, E., Magana, V., Zitacuaro, A., Cardenas, B., Retama, A., Ramos, R., Molina, L. T., and Molina, M. J.: Mexico City basin wind circulation during the MCMA-2003 field campaign, Atmos. Chem. Phys., 5, 2267–2288, 2005, http://www.atmos-chem-phys.net/5/2267/2005/.

de Foy, B., Clappier, A., Molina, L. T., and Molina, M. J.: Distinct wind convergence patterns due to thermal and momentum forcing of the low level jet into the Mexico City basin, Atmos. Chem. Phys., 6, 1249–1265, 2006, http://www.atmos-chem-phys.net/6/1249/2006/.

de Foy, B., Lei, W., Zavala, M., Volkamer, R., Samuelsson, J., Mellqvist, J., Galle, B., Martínez, A.-P., Grutter, M., Retama, A., and Molina, L. T.: Modelling constraints on the emission inventory and on vertical dispersion for CO and SO2 in the Mexico City Metropolitan Area using Solar FTIR and zenith sky UV spectroscopy, Atmos. Chem. Phys., 7, 781–801, 2007, http://www.atmos-chem-phys.net/7/781/2007/.

ENVIRON: User's Guide: Comprehensive Air Quality Model with Extension (CAMx), ENVIRON International Coporation, Novato, California, Version 4.03, 2003.

Kleinman, L. I., Daum, P. H., Lee, J. H., Lee, Y.-N., Nunnermacker, L. J., Springston, S. R., Newman, L., Weinstein-Lloyd, J., and Sillman, S.: Dependence of ozone production on NO and hydrocarbons in the troposphere, Geophys. Res. Lett., 24, 2299–2302, 1997.

Kolb, C. E., Herndon, S. C., McManus, J. B., Shorter, J. H., Zahniser, M. S., Nelson, D. D., Jayne, J. T., Canagaratna, M. R., and Worsnop, D. R.: Mobile laboratory with rapid response instruments for real-time measurements of urban and regional trace gas and particulate distributions and emission source characteristics, Environ. Sci. Technol., 38, 5694–5703, 2004.

Lei, W., de Foy, B., Zavala, M., Volkamer, R., and Molina, L. T: Characterizing ozone production in the Mexico City Metropolitan Area: a case study using a chemical transport model, Atmos. Chem. Phys., 7, 1347–1366, 2007, http://www.atmos-chem-phys.net/7/1347/2007/.

Liu, S. C., Trainer, M., Fehsenfeld, F. C., Parrish, D. D., Williams, E. J., Fahey, D. W., Hubler, G., and Murphy, P. C.: Ozone production in the rural troposphere and the implications for regional and global ozone distributions, J. Geophys. Res., 92, 4191–4207, 1987.

Molina, L. T., Kolb, C. E., de Foy, B., Lamb, B. K., Bruce, W. H., Jimenez, J. L., Ramos-Villegas, R., Sarmiento, J., Paramo-Figueroa, V. H., Cardenas, B., Gutierrez-avedoy, V., and Molina, M. J.: Air quality in North America's most populous city-overview of MCMA-2003 Campaign, Atmos. Chem. Phys., 7, 2447–2473, 2007, http://www.atmos-chem-phys.net/7/2447/2007/.

Molina, L. T. and Molina, M. J. (Eds.): Air Quality in the Mexico Megacity: An Integrated Assessment, Kluwer Academy Publishers, 2002.

Molina, M. J. and Molina, L. T.: Megacities and Atmospheric Pollution, J. Air Manage. Assoc., 54, 644–680, 2004.

NRC (National Research Council): The effects of meteorology on tropospheric ozone, in: Rethinking the Ozone Problem in Urban and Regional Air Pollution, National Academy Press,

Washington DC, USA, 93–108, 1991.
Seaman, N. L.: Meteorological modeling for air-quality assessments, Atmos. Environ., 34, 2231–2258, 2000.
Sillman, S: The use of NO_y, H_2O_2, and HNO_3 as indicators for ozone-NO_x-hydrocarbon sensitivity in urban locations, J. Geophys. Res., 100, 14 175–14 188, 1995.
Sillman, S.: The relation between ozone, NO_x and hydrocarbons in urban and polluted rural environments, Atmos. Environ., 33, 1821–1845, 1999.
SIMAT: Sistema de Monitoreo Atmosferico, Ciudad de Mexico, http://www.sma.df.gob.mx/simat/, 2003.
Solomon, P., Cowling, E., Hidy, G., and Furiness, C.: Comparison of scientific findings from major ozone field studies in North America and Europe, Atmos. Environ., 34, 1885–1920, 2000.
Velasco, E., Lamb, B., Westberg, H., Allwine, E., Sosa, G., Arriaga, J. L., Jonson, T., Alexander, M., Prazeller, P., Knighton, B., Rogers, T. M., Grutter, M., Herndon, S. C., Kolb, C. E., Zavala, M., de Foy, B., Molina, L. T., and Molina, M. J.: Distribution, magnitudes, reactivities, ratios and diurnal patterns of volatile organic compounds in the Valley of Mexico during the MCMA 2002 & 2003 field campaigns, Atmos. Chem. Phys., 7, 329–353, 2007, http://www.atmos-chem-phys.net/7/329/2007/.
Volkamer, R., Molina, L. T., Molina, M. J., Shirley, T., and Brune, W. H.: DOAS measurement of glyoxal as an indicator for fast VOC chemistry in urban air, Geophys. Res. Lett., 32, L08806, doi:10.1029/2005GL022616, 2005.
Willmott, C. J.: On the validation of models, Phys. Geogr., 2, 184–194, 1981.
Zavala, M., Slott, R., S, Dunlea, E. J., Marr, L., Molina, L. T., Molina, M. J., Herndon, S. C., Shorter, J. H., Zahniser, M., Kolb, C. E., Knighton, B., and Rogers, T: Characterization of on-road vehicle emissions in the Mexico City Metropolitan Area using a mobile laboratory in chase and fleet average measurement modes during the MCMA-2003 field campaign, Atmos. Chem. Phys., 6, 5129–5142, 2006, http://www.atmos-chem-phys.net/6/5129/2006/.

Table 1. Adjustment factors for corrections of the 2002 and 2004 MCMA emissions inventory

CAMx Model species	Adjustment factor
CO	0.9–1.1
NO_x	0.9–1.1
ALK1	2.0–3.0
ALK2	2.5–3.5
ALK3	3.0–4.0
ALK4	1.2–1.5
ALK5	0.4–0.6
ETHE	1.0–1.3
OLE1	0.8–1.0
OLE2	0.7–1.0
ARO1	1.2–1.5
ARO2	1.0–1.5
HCHO	5.0–9.0
CCHO and RCHO	4.0–9.0

Table 2. Model statistical performance measures in the MCMA

			O_3*	CO	NO_y
Cold Surge	Mean obs	(ppb)	27.1	1887	80.9
	Mean mdl	(ppb)	26.4	1642	75.5
	RMSE	(ppb)	18.9	1313	55.3
	IOA		0.88	0.78	0.80
	NB	(%)	−5.6	49.4	33.4
	NGE	(%)	30.6	86.5	66.6
	NMB	(%)	−9.5	−13.1	−6.3
	AAP	(%)	7.5	−11.6	−4.3
O_3 South	Mean obs	(ppb)	47.5	1273	61.0
	Mean mdl	(ppb)	42.7	1379	60.6
	RMSE	(ppb)	21.6	925	43.0
	IOA		0.93	0.76	0.79
	NB	(%)	−1.7	71.5	30.3
	NGE	(%)	24.6	97.2	63.8
	NMB	(%)	−1.3	8.2	−1.1
	AAP	(%)	8.9	28.6	10.1
O_3 North	Mean obs	(ppb)	45.8	1884	84.2
	Mean mdl	(ppb)	41.0	1894	83.8
	RMSE	(ppb)	24.9	1277	58.3
	IOA		0.92	0.77	0.81
	NB	(%)	−5.6	47.9	36.4
	NGE	(%)	28.3	79.3	68.4
	NMB	(%)	−5.9	0.6	−0.4
	AAP	(%)	3.2	15.0	2.0

Obs = observation. Mdl = model. RMSE = root mean square error, IOA = index of agreement (Willmott, 1981), NB = normalized bias, NGE = normalized gross error, NMB = normalized mean bias, AAP = average accuracy of peak paired in site. *: In the calculation of NB, NGE and NMB for O_3, the threshold value for observed O_3 was set to 40 ppb.

ACPD
8, 12053–12079, 2008

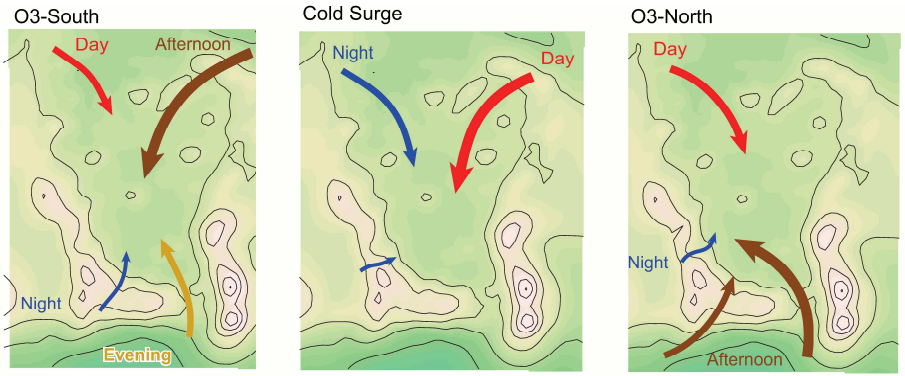

Fig. 1. Circulation model for the Mexico City basin for O_3-South, Cold Surge and O_3-North. Arrows colored by time of day are dominant wind flows. Weak drainage flows on O_3-South days give way to strong north-easterly winds. A weak southerly jet forms in the Chalco passage in the evening. Cold Surge days have predominantly northerly flow with a westerly component at night turning to easterly flow from the Gulf in the afternoon. On O_3-North days, the day-time flow is from the north-west and gives way to a strong afternoon jet that starts in the pass but expands over the entire southern basin rim. Figure from de Foy et al. (2005).

ACPD
8, 12053–12079, 2008

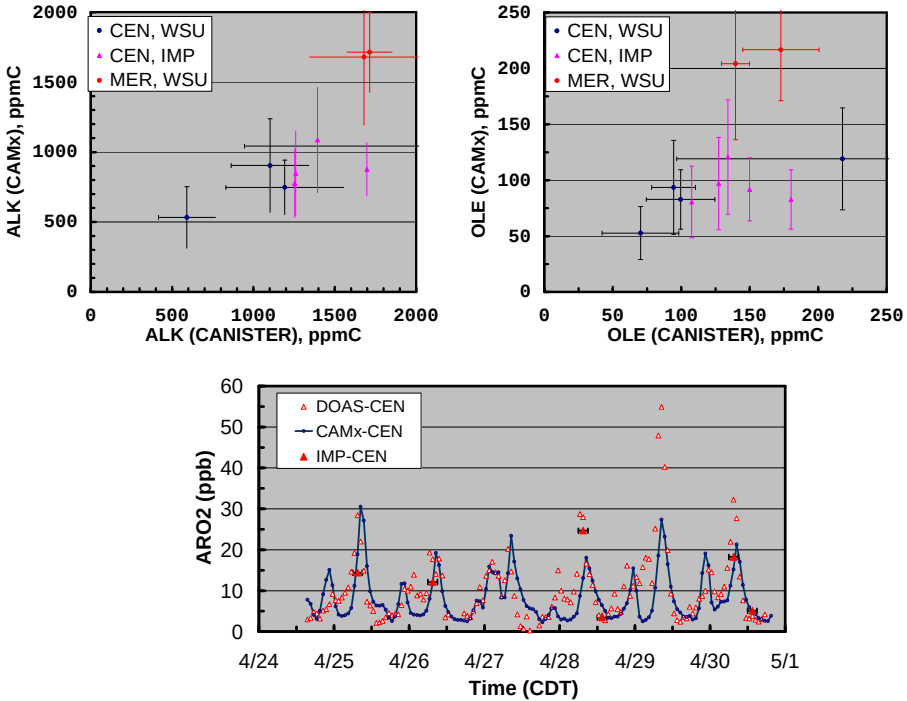

Fig. 2. Comparisons of modeled VOC concentrations with Canister (upper panel, 06:00–09:00 CDT average) and DOAS (lower panel) measurements after EI VOCs were adjusted.

ACPD
8, 12053–12079, 2008

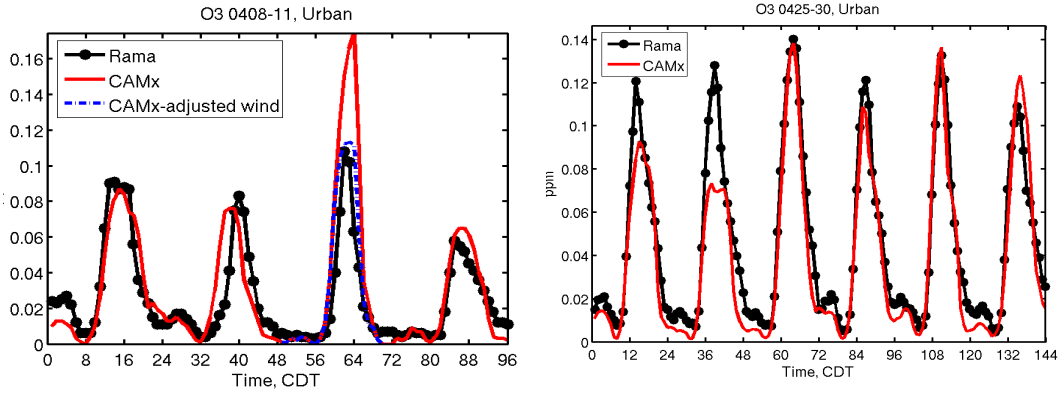

Fig. 3. Comparison of measured (black) and simulated (red) diurnal variation of near surface O_3 concentrations averaged over the urban area (21 monitoring stations) during the "Cold Surge" (8–11 April, left) and the "O_3-North" (25–30 April, right) episodes. Also shown in the left panel are the simulated O_3 concentrations (blue dashed) on 10 April when the gap flow was enhanced by 0.5 m/s.

ACPD
8, 12053–12079, 2008

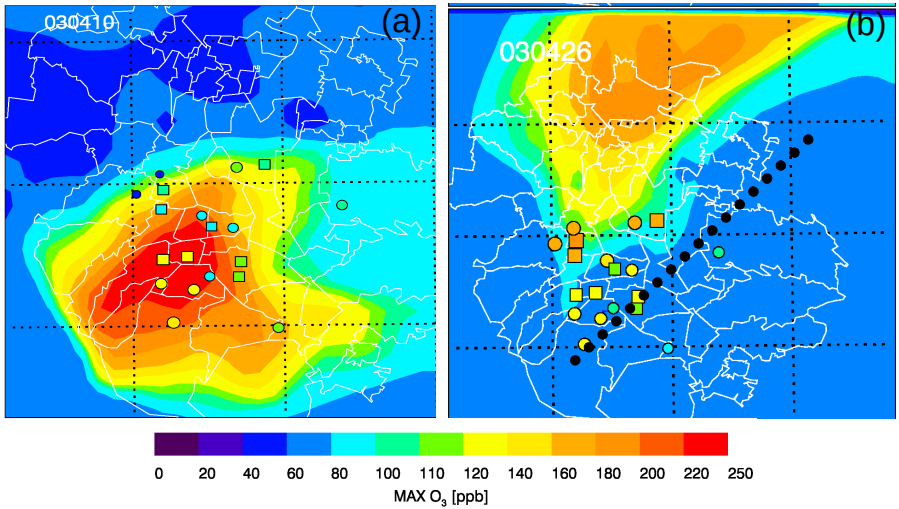

Fig. 4. Comparison of simulated (colored contour) versus observed (colored dots and squares) geographical distribution of near-surface peak O_3 concentration on **(a)** 10 April and **(b)** 26 April 2003. The dotted line in (b) is the cross-section which approximated the average transport pathway of the urban plume during this O_3-North episode.

ACPD
8, 12053–12079, 2008

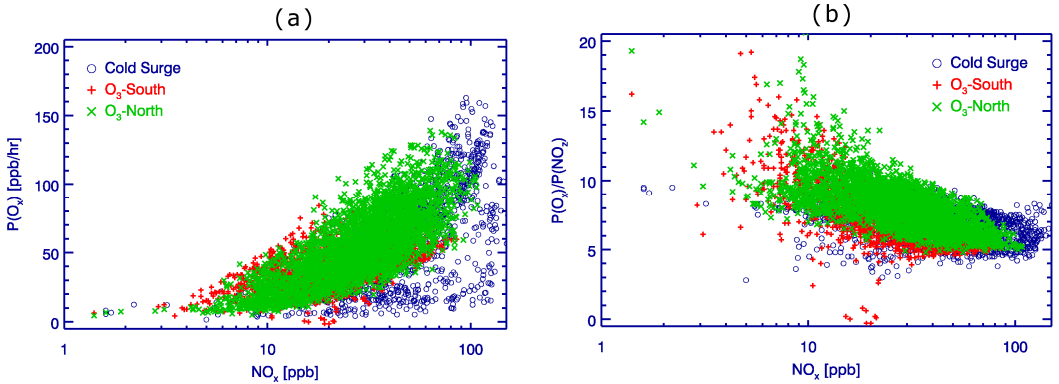

Fig. 5. Simulated midday (12:00–17:00 LT) net O_x production rate (left) and O_3 production efficiency (right) as a function of NO_x concentration in the urban area of MCMA under different meteorological conditions.

ACPD
8, 12053–12079, 2008

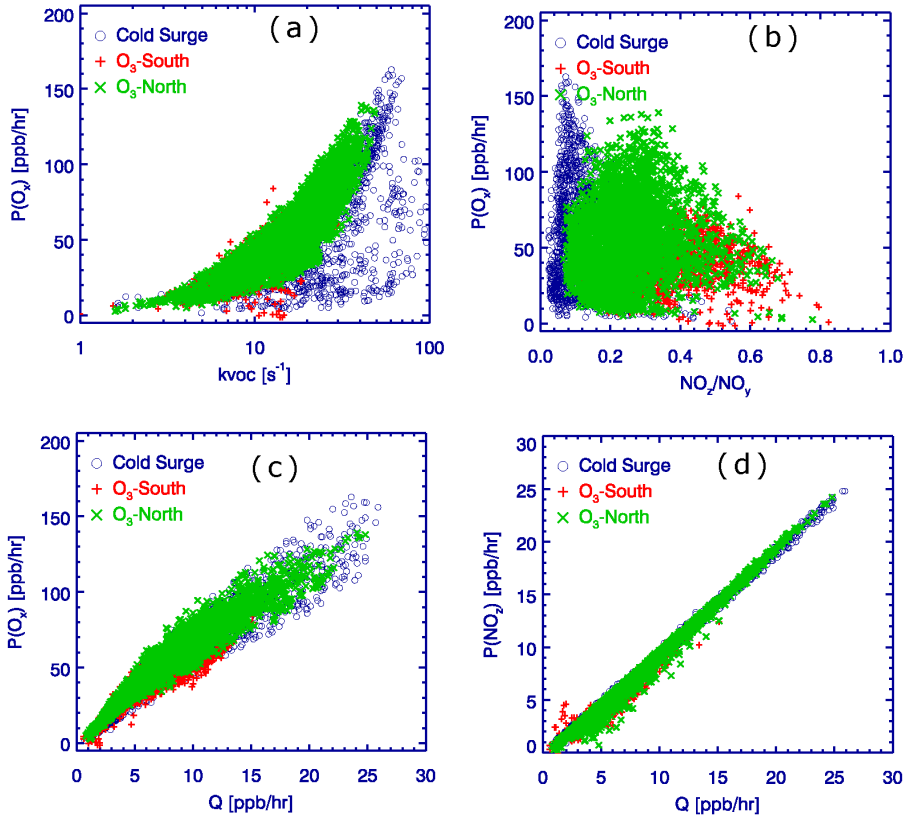

Fig. 6. Simulated relationship among $P(O_x)$, VOC reactivity (k_{VOC}), chemical aging (NO_z/NO_y) in the urban area between 12:00–17:00 CDT during different meteorological conditions.

ACPD
8, 12053–12079, 2008

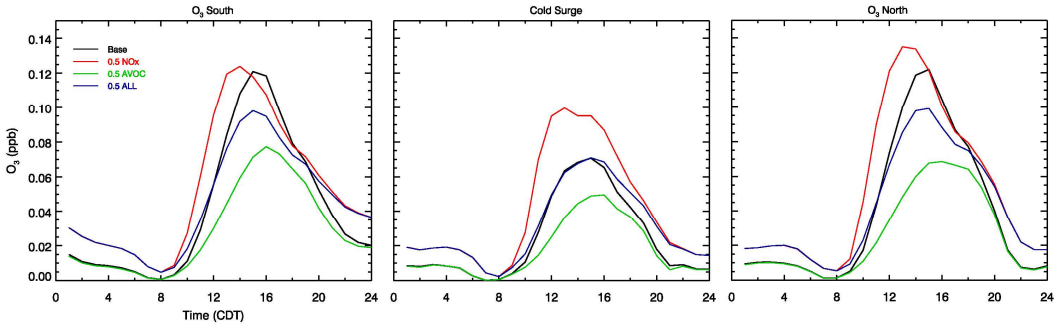

Fig. 7. Time series of surface O_3 concentrations for different emission control scenarios under different meteorological conditions. Data are averaged over 8 urban representative monitoring stations and over each episode. In the legend Base denotes the base case, 0.5 NO denotes a 50% reduction in NO_x emissions, 0.5 VOC a 50% reduction in VOC emissions, and 0.5 ALL a 50% reduction in both NO_x and VOC emissions.

ACPD
8, 12053–12079, 2008

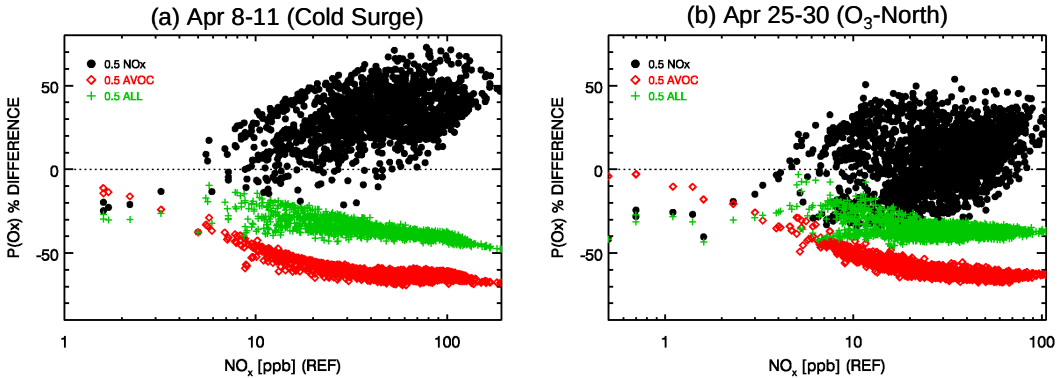

Fig. 8. The percentage change of $P(O_x)$ as a function of NO_x from 13:00–17:00 CDT during **(a)** the "Cold Surge" and **(b)** the "O_3-North" episodes in the MCMA urban region.

ACPD
8, 12053–12079, 2008

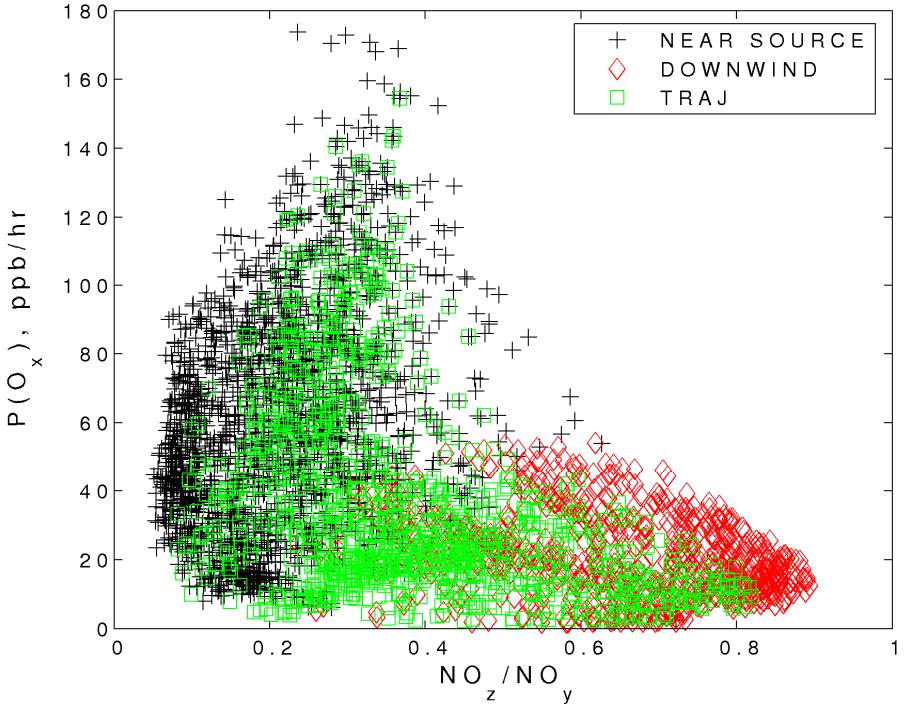

Fig. 9. Relationship between $P(O_x)$ and chemical aging (NO_z/NO_y) during 12:00–17:00 CDT, 25–30 April 2003. Black dots are data sampled in the downtown near the source area, red diamonds are data sampled about 60 km downwind of the urban core, and blue squares are data sampled along a 3-grid-wide band along the cross section in Fig. 4.

ACPD
8, 12053–12079, 2008

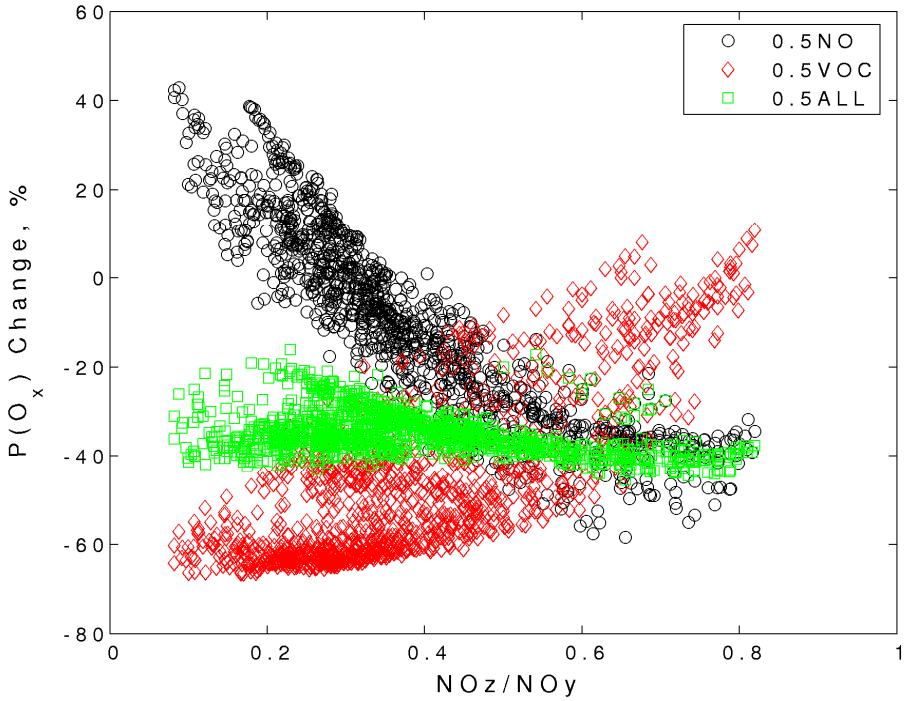

Fig. 10. Percentage change of $P(O_x)$ as a function of chemical aging along the plume transport pathway during 25–30 April 2003 when emissions of NO_x and VOCs are reduced by 50% each and both.

ACPD
8, 12053–12079, 2008